

# Effect of carbon contents on microstructure of B<sub>4</sub>C/SiC composites

XIAO-JU GAO<sup>a,b</sup>, LAI-FEI CHENG<sup>a</sup>, JIAN-WU CAO<sup>b</sup>, DONG-MING YAN<sup>b,c</sup>, CONG ZHANG<sup>b</sup>, PENG MAN<sup>b</sup>, JUN-FENG QU<sup>b</sup>, YA-WEI ZHOU<sup>b</sup>, SU-JIE SUN<sup>b</sup>

<sup>a</sup>Science and Technology on Thermostructural Composite Materials Laboratory, Northwestern Polytechnical University, Xi'an 710072, China

<sup>b</sup>No. 52 Institute of China North Industry Group, Yantai 264003, China

<sup>c</sup>Yantai Jinli New Materials Co., Ltd

B<sub>4</sub>C/SiC composites were obtained by reaction sintering between C/B<sub>4</sub>C green body and liquid Si, and the effect of carbon contents on microstructure was investigated by OM and SEM. Results show that B<sub>4</sub>C/SiC composites consist of three new phases, namely, SiC, B<sub>13</sub>C<sub>2</sub>, and B<sub>12</sub>(C, Si, B)<sub>3</sub>. Compared with composites without carbon addition, microstructure becomes more even and smaller with increased carbon contents ranging from 0 vol.% to 10 vol.%, which may be due to the generation of a small amount of SiC and the increase in grain boundary. However, when the carbon contents exceeded 10 vol.%, residual carbon can form defects, and abnormal grain growth is clearly observed. Meanwhile, increased carbon addition, more SiC is generated results in poor distribution uniformity of each phase.

(Received December 31, 2014; accepted March 19, 2015)

**Keywords:** SiC/B<sub>4</sub>C composite, Reaction sintering, Microstructure, Abnormal grain growth

## 1. Introduction

B<sub>4</sub>C ceramic has long been considered as a choice for armor and nuclear protection fabrication fields as a result of good ballistic and wear resistance, higher hardness and modulus, lower density, and higher thermal neutron shielding factor [1-4]. However, its low fracture toughness has impeded wider applications on certain structural components. Adding SiC to B<sub>4</sub>C-based materials is an effective method of obtaining relatively higher fracture toughness, while preserving the good mechanical and physical properties of B<sub>4</sub>C [5,6].

Li Aiju [7] has recently obtained B<sub>4</sub>C/SiC composites by hot pressing technology under a temperature ranging between 1800 °C to 1880 °C and pressure of 30 MPa, and the relative density of the obtained composite material was 95.6%. Furthermore, Masato Uehara [8] fabricated composites by hot pressing technology at a temperature of 2000 °C without any sintering additives, and the relative density of the obtained composite material was 99%. However, disadvantages of the composites, which include high sintering temperature and cost, limit wider use. By contrast, reaction sintering to obtain B<sub>4</sub>C/SiC composites has been considered as an alternative method because of shorter sintering time and lower sintering temperature, as well as lower cost, in particular, to obtain higher density.

Hayun [9] added free carbon to B<sub>4</sub>C by sugar pyrolysis and fabricated the composite material by reaction sintering with molten Si. However, the

microstructure of the composites has yet to be studied systematically. In this paper, reaction sintering was used to fabricate the B<sub>4</sub>C/SiC composites at a lower temperature, and the material components and a theory of formulation were developed. In addition, the study aims to study the influence of different carbon addition amounts on the microstructures of composites, to provide more theoretical basis and support for the study of mechanical properties in the future.

## 2. Experimental procedure

### 2.1 Fabrication of Composites

(1) B<sub>4</sub>C powder (5 μm, Jin Ma Company) and carbon powder (Yi Jia Chemical Co.), along with a certain amount of binders, were uniformly mixed based on Table 1. Then, the mixtures were mechanically ball-milled in ethanol for 12 h using agate balls and dried at 65 °C for 12 h.

Table 1. Formation of SiC/B<sub>4</sub>C composition.

Samples	0#	1#	2#	3#
C (vol. %)	0%	5%	10%	15%
B <sub>4</sub> C (vol. %)	100%	95%	90%	85%

(2) After being dried, crushed and screened through a 200 mesh sieve, the powders were granulated. The mixture was placed into the mold and compacted by die-pressing (SL-45, Shanghai Mechanics, China) at 120 MPa.

(3) The green bodies were infiltrated with liquid silicon at 1650 °C for 2 h under  $1 \times 10^{-3}$  Pa vacuum in vacuum sintering furnace.

## 2.2 Microstructure and composition

Porosity was measured by mercury intrusion method. Density was determined by the water immersion technique in accordance with ASTM Standard.B311. The phase composition and structure of the samples were analyzed by X-ray diffraction (XRD). The microstructure of the composites was characterized by optical microscope (OM

2000) and scanning electron microscope (SEM, SEM 4800).

## 3. Results and discussion

### 3.1 Composition design

In the reaction-bonded SiC/B<sub>4</sub>C composite, B<sub>4</sub>C and Si at the temperature of the experiment are inert because the wetting angle of Si to B<sub>4</sub>C is 0°. The reaction-bonding mechanism is the same as that for the reaction bonded silicon carbide silicon carbide (RBSC). The process of the reaction-bonded SiC/B<sub>4</sub>C is shown in Fig. 1.

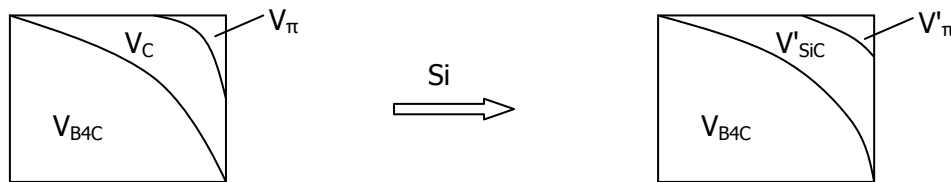


Fig. 1. Schematic of the reaction-bonded SiC/B<sub>4</sub>C.

( $V_\pi$  is the pore volume of a green body;  $V'_\pi$  is the pore volume of a sintered body).

In the preparation of the SiC/B<sub>4</sub>C composite without any obstruction of infiltrating Si, the main reaction involved is  $C+Si \rightarrow SiC$ . The atomic weights of C and SiC are known, and the volume ratio of SiC/C in the ingredients can be determined from the theoretical densities of C and SiC, which are calculated as follows:

$$\frac{V'_{SiC}}{V_C} = \frac{\frac{M_{SiC}}{\rho_{SiC}}}{\frac{M_C}{\rho_C}} = 2.33 \quad (1)$$

Based on this calculation, the equation can be developed as follows:

$$V'_{SiC} = 2.33V_C \quad (2)$$

Normally, a sintered body of RBSC consists only of SiC and Si and is free of pores and carbon residue. If the volume of a green body is equal to that of a sintered body and considering the mass conservation law, the equation obtained is as follows:

$$V_C + V_\pi = V'_{SiC} + V'_\pi \rightarrow V_C + V_\pi = 2.33V_C + V' \quad (3)$$

$$1.33V_C = V_\pi - V'_\pi \quad (4)$$

Ideally, the composite is free of residual silicon ( $V'_\pi = 0$ ). Based on the testing,  $V_\pi$  is 0.35, and the volume fraction of carbon is calculated as follows:

$$V_C = \frac{V_\pi - V'_\pi}{1.33} = 26.32\% \quad (5)$$

Namely, the carbon contents of the reaction-bonded SiC/B<sub>4</sub>C system formulations should theoretically range from 0 to 26.32 vol%. Combine with previous research outcome on its mechanical properties [10], effect of carbon contents ranged from 0 to 15 vol% on the microstructure of SiC/B<sub>4</sub>C will be studied in this paper.

### 3.2 Composition of B<sub>4</sub>C/SiC composites

Fig. 2 shows the XRD patterns of B<sub>4</sub>C/SiC composites with varied C contents. We can see new phases, which included SiC, B<sub>13</sub>C<sub>2</sub>, and B<sub>12</sub>(C, Si, B)<sub>3</sub> in the B<sub>4</sub>C/SiC composites, in comparison with composites fabricated by reaction sintering without any carbon. In addition, residual Si can be detected in composites with or without carbon addition.

With increased carbon contents, particularly at 15 vol. % C, residual carbon can be detected within the material system, indicating an incomplete reaction and excess of carbon. This phenomenon may be due to greater SiC amount generated in the reaction of molten silicon and carbon powder, which surrounds the carbon powder and hinder the reaction of carbon and silicon. However, residual carbon may cause a decline in the strength of the sintered body because of the zero strength [11].

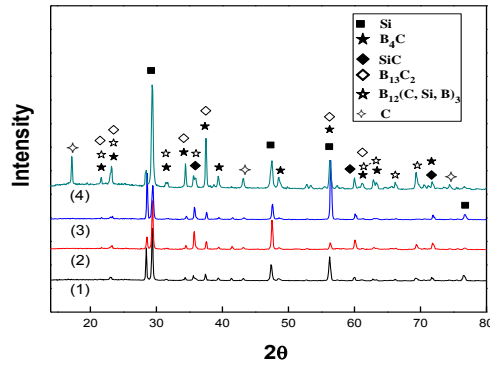


Fig. 2. XRD patterns of  $B_4C/SiC$  composites with various C contents: (1) 0 vol. %; (2) 5 vol. %; (3) 10 vol. %; (4) 15 vol. %.

### 3.3 Compactness of $B_4C/SiC$ composites

Fig. 3 shows the density and porosity of composites with different contents of carbon. As can be seen in Fig. 3, higher carbon contents translated to higher density of the composites, all four group of samples have better compactness because of the lower porosity. However, a carbon contents exceeding 10 vol.% results in gradually increased the amplitude of density. Meanwhile, porosity presents a minimum with increased carbon addition. Adding a certain amount of carbon powder can lead to the formation of SiC. Pores can be filled, and porosity consequently decreases. However, when carbon addition exceeds 10 vol.%, SiC particles tend to aggregate together in the reaction progress and partially blocks the channels of silicon infiltration. This blockage result in pores within composites, and thus porosity increases [12].

With increased carbon contents, the relative contents of SiC in composites increases because of the higher density of SiC ( $3.21 \text{ g/cm}^3$ ) than  $B_4C$  ( $2.52 \text{ g/cm}^3$ ). Increased carbon contents definitely lead to increased density of the composites. In addition, the porosity decline leads to the increased compactness and contributes to the increase of density. However, beyond 10 vol.% C, the increase in porosity affects the increase in density.

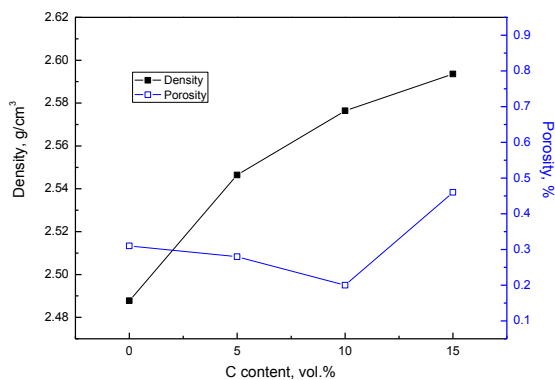


Fig. 3. Density and porosity of  $B_4C/SiC$  composites with various C contents (1) 0 vol. %; (2) 5 vol. %; (3) 10 vol. %; (4) 15 vol. %.

### 3.3 Microstructure of $B_4C/SiC$ composites

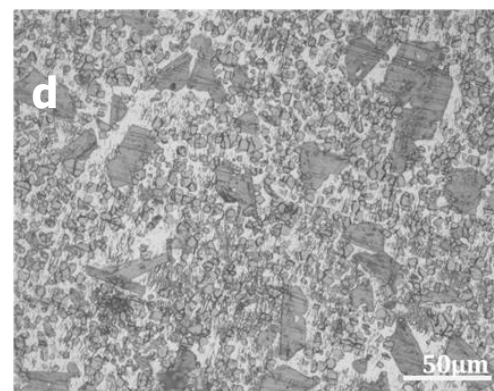
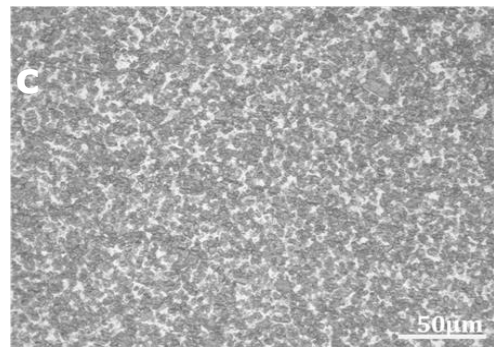
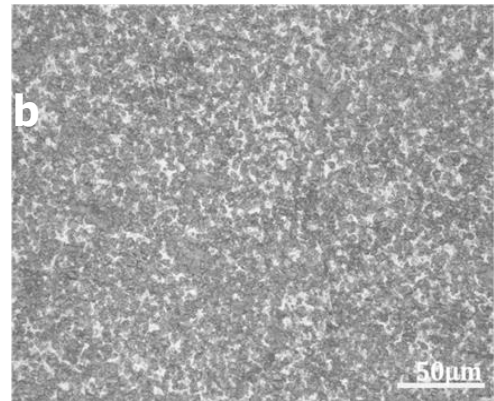
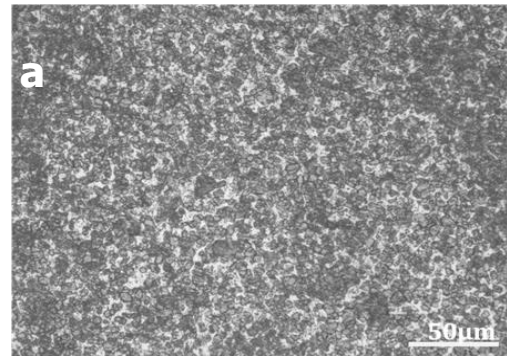


Fig. 4. OM images of  $SiC/B_4C$  composites with different C contents: (a) 0 vol. %; (b) 5 vol. %; (c) 10 vol. %; (d) 15 vol. %.

Fig. 4 shows the OM images of the composites with different carbon contents. In Fig. 3, without any addition of carbon, the distribution of grains within sintering body is uneven (Fig. 4(a)). Particles are dispersed unevenly, which suggests the significant agglomeration of the powder in the process of mixing. In contrast, the addition of carbon results in greater uniform distribution of grains, and particles are dispersed more evenly with increased carbon contents from 0 vol.% to 10 vol.%. In addition, no abnormal grain growth [13–15] is found when carbon addition ranged between 0 and 10 vol.%, which may be due to the generation of a small amount of SiC and the increase in grain boundary.

However, when carbon content is higher than 10 vol. %, more non-uniform grain distribution is observed. Abnormal grain growth is clearly seen in Fig. 4(d). Given the higher carbon contents, more SiC is generated, which enhances the thermal effect, bridges B<sub>4</sub>C particles, and ultimately promotes abnormal grain growth.

Fig. 5 shows the SEM images of B<sub>4</sub>C/SiC composites. We used Fig. 5 in combination with the EDS analysis (Fig. 6) to define A, B, C, D, and E, which respectively stands for different phases. Gray-colored area A is a mixing zone with less SiC and more Si. Black-colored area B approximates the B<sub>4</sub>C phase. Area C, which is also of a gray color, is a mixing zone of less Si and more SiC, which is the same as in areas D and F, only varying according to the atomic ratio of C/Si.

According to Fig. 5(a), without carbon addition, the composite material mainly consists of Si and B<sub>4</sub>C phase. However, a small amount of binder mixed with carbon element, which was added to the original powder in the process of mixing materials, caused the reaction between Si and C and lead to the formation of less SiC. Thereby, a mixing zone of less SiC and more Si appears among the B<sub>4</sub>C phases with a dispersive distribution. In contrast, the element of gray areas transforms from a region containing more Si to a region containing more SiC with the addition of carbon powder. This transformation is attributed to the complete reactions between molten silicon and carbon, leading to the formation of more SiC molecules. Meanwhile, the molten silicon continues to infiltrate and surround SiC. Finally, a mixing zone of less Si and more SiC forms (Fig. 5(b)).

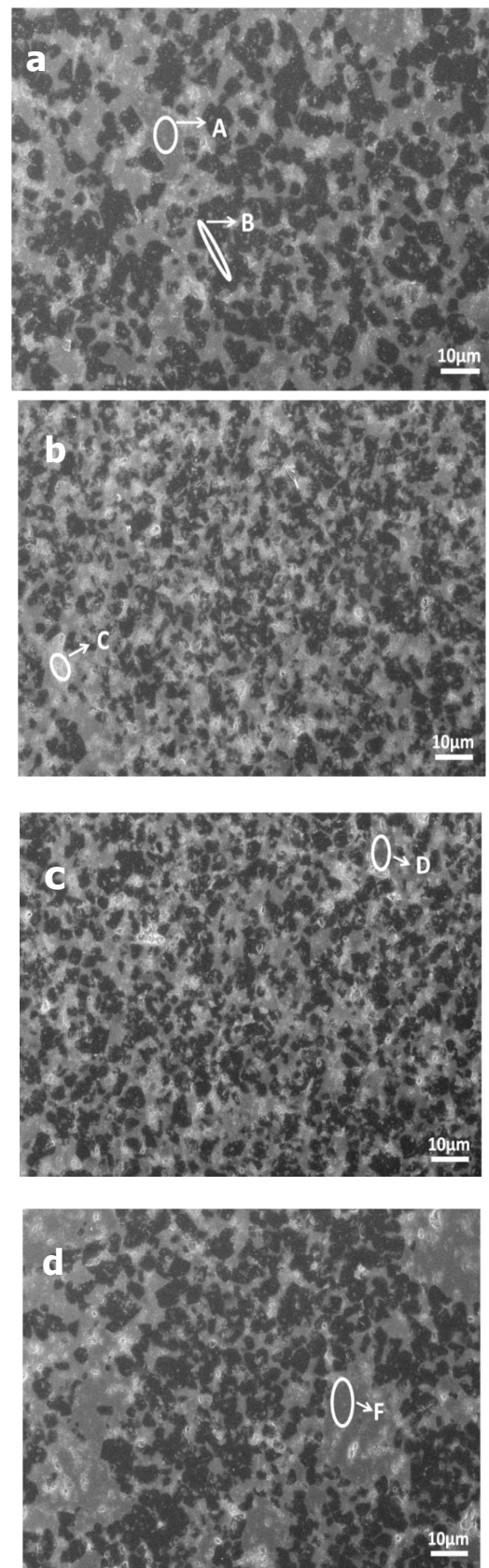


Fig. 5. SEM images of SiC/B<sub>4</sub>C composites with different C contents: (a) 0 vol. %; (b) 5 vol. %; (c) 10 vol. %; (d) 15 vol. %.

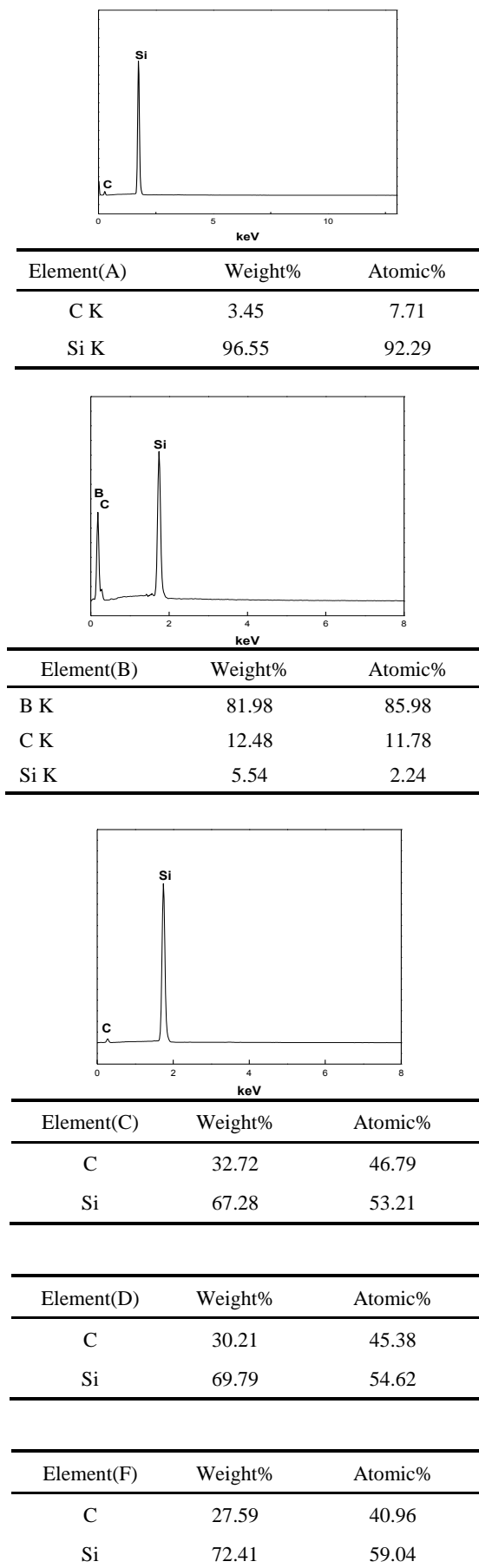


Fig. 6. EDS analysis of composites.

In addition, we can see that, without carbon addition, phases display various sizes, which is due to the difficulty of  $B_4C$  sintering without any sintering aids [16]. More carbon addition beyond 10 vol.% carbon results in poorer distribution uniformity of each phase, because a high ratio of SiC is generated in the reaction, and agglomeration result in regions with larger size (Fig. 5(d)).

#### 4. Conclusions

(1) In comparison with composites fabricated by reaction sintering without any carbon addition, new phases, which include SiC,  $B_{13}C_2$ , and  $B_{12}(C, Si, B)_3$ , can be detected in  $B_4C/SiC$  composites with carbon addition. At a carbon contents exceeding 10 vol.%, residual carbon appears.

(2) The addition of carbon results in more uniform distribution of grains, and particles are dispersed more evenly with increased carbon contents. However, when the carbon contents is higher than 10 vol.%, abnormal grain growth is evidently observed.

(3) Combined with SEM and EDS analysis, the element of the phase with grey color transforms from the region containing more Si to the region containing more SiC with the addition of carbon powder, which confirms the generation of SiC.

#### References

- [1] M. K. Aghajanian, B. N. Morgan, J. R. Singh, et al. *Ceramic transactions*, **134**, 527 (2002).
- [2] W. G. Zhang, H. M. Cheng, H. Sano, et al. *Carbon*, **36**(11), 1591 (1998).
- [3] H. W. Kim, Y. H. Koh, H. E. Kim, *Journal of the American Ceramic Society*, **83**(11), 2863 (2000).
- [4] V. Kulikovskiy, V. Vorlicek, P. Bohac, et al. *Diamond and Related Materials*, **18**, 27 (2009).
- [5] R. M. da Rocha, F. C. L. de Melo, *Ceramic Engineering and Science Proceedings* **30**(5), 113 (2009).
- [6] M. Uehara, R. Shiraishi, A. Nogami, et al, *Journal of the European Ceramic Society*, **24**(2), 409 (2004).
- [7] Li Aiju, Yin Yansheng, Zhen Yuhua, et al. *Journal of Composite Materials*, **21**(4), 129 (2004).
- [8] M. Uehara, R. Shiraishi, A. Nogami et al. *Journal of the European Ceramic Society*, **24**, 409 (2004).
- [9] S. Hayun, Dilman H, Dariel M P, et al. *Advances in Sintering Science and Technology: Ceramic Transactions*, 29-39 (2010).
- [10] X. J. Gao, et al. *Journal of Inorganic Materials* (2014), DOI: 10.15541/jim20140494.
- [11] H. Qingwei, Q. Guanjuan, G. Jiqiang, et al. *Rare Metal Materials and Engineering*, **30**(2; ISSU 187), 149 (2001).

- 
- [12] G. Arslan, A. Kalemantas, *Journal of the European Ceramic Society*, **29**(3), 473 (2009).
- [13] H. Chun, S. Na, J. Yoo, et al. *Journal of Applied Physics*, 2011, 109(7).
- [14] I. Bae, S. Baik, *Journal of the American Ceramic Society*, **80**(5), 1149 (1997)
- [15] A. M. Kueck, L. C. D. Jonghe, *Journal of the European Ceramic Society*, **28**, 2259 (2008).
- [16] H. W. Kim, Y. H. Koh, H. E. Kim, *Journal of the American Ceramic Society*, **83**(11), 2863 (2000).

---

\*Corresponding author: chenglf@nwpu.edu.cn